Neuron
Article

An Instructive Role for Patterned Spontaneous Retinal Activity in Mouse Visual Map Development

Hong-ping Xu,[1,*] Moran Furman,[1] Yann S. Mineur,[2] Hui Chen,[3,6] Sarah L. King,[2] David Zenisek,[3,4] Z. Jimmy Zhou,[3,4] Daniel A. Butts,[5] Ning Tian,[1,3,6] Marina R. Picciotto,[1,2] and Michael C. Crair[1,3,*]
[1]Department of Neurobiology
[2]Department of Psychiatry
[3]Department of Ophthalmology and Visual Science
[4]Department of Cellular and Molecular Physiology
Yale University School of Medicine, New Haven, CT 06510, USA
[5]Department of Biology and Program in Neuroscience and Cognitive Science, University of Maryland, College Park, MD 20742, USA
[6]Present address: Department of Ophthalmology, University of Utah School of Medicine, Salt Lake City, UT 84132, USA
*Correspondence: hong-ping.xu@yale.edu (H.-p.X.), michael.crair@yale.edu (M.C.C.)
DOI 10.1016/j.neuron.2011.04.028

SUMMARY

Complex neural circuits in the mammalian brain develop through a combination of genetic instruction and activity-dependent refinement. The relative role of these factors and the form of neuronal activity responsible for circuit development is a matter of significant debate. In the mammalian visual system, retinal ganglion cell projections to the brain are mapped with respect to retinotopic location and eye of origin. We manipulated the pattern of spontaneous retinal waves present during development without changing overall activity levels through the transgenic expression of β2-nicotinic acetylcholine receptors in retinal ganglion cells of mice. We used this manipulation to demonstrate that spontaneous retinal activity is not just permissive, but instructive in the emergence of eye-specific segregation and retinotopic refinement in the mouse visual system. This suggests that specific patterns of spontaneous activity throughout the developing brain are essential in the emergence of specific and distinct patterns of neuronal connectivity.

INTRODUCTION

The development of precise patterns of neural connectivity characteristic of the mammalian brain is thought to occur through a combination of molecular and neuronal activity-dependent mechanisms (Goodman and Shatz, 1993; Cline, 2003). During late stages of mammalian brain development, sensory-driven neuronal activity profoundly shapes neural circuit structure and function so that manipulating sensory experience (e.g., through monocular deprivation) can produce dramatic shifts in neural response properties and corresponding changes in neural circuits during "critical periods" of development. In contrast, during early stages of brain development, molecular factors directly regulate cell survival, neurite outgrowth, and branch formation. While it is generally accepted that during these early stages of development neuronal activity can modulate brain development (Spitzer, 2006), it remains remarkably controversial whether this early neuronal activity acts only in a passive way to trigger downstream signaling pathways that promote neuron development (Chalupa, 2009; Sun et al., 2008; Huberman et al., 2003) or whether it can act in an instructive way to guide neural circuit formation through specific spatiotemporal patterns of neural activity (Feller 2009; Huberman et al., 2008).

These issues have been investigated in some detail in the mammalian visual system, where retinal ganglion cell (RGC) projections to the dorsal lateral geniculate nucleus (dLGN) and superior colliculus (SC) form two sensory maps, one reflecting eye of origin and the other retinotopic location (Huberman et al., 2008). Molecular factors are clearly involved in forming these neural circuits, directing RGC axons whether to cross at the optic chiasm (Petros et al., 2008) and where to branch in the dLGN and SC (Huberman et al., 2008; McLaughlin and O'Leary, 2005). Evidence concerning the role of neuronal activity in early visual map development is more equivocal, failing to distinguish whether neuronal activity acts in a passive way to promote cell survival and neurite outgrowth, or in an instructive way to guide neural circuit formation through specific spatiotemporal patterns of neural activity (Crair, 1999; Stellwagen and Shatz, 2002; Huberman et al., 2003). This fundamental question has been difficult to answer because manipulations that change the spatiotemporal pattern of ongoing spontaneous neuronal activity typically also alter the activity of individual neurons (their overall spike rate, or burst frequency, etc.). This completely confounds changes in interneuronal activity patterns with changes in single-neuron activity levels, making it impossible to distinguish between a passive and active role for neuronal activity in visual map development (Chalupa, 2009; Feller, 2009).

As in many parts of the developing brain and spinal cord (Meister et al., 1991; Bekoff et al., 1975; Feller, 1999), coordinated waves of spontaneous neuronal activity are found in the retina of all mammalian species examined (Wong, 1999; Warland et al., 2006), well before the onset of sensory experience. Maps

for eye of origin and retinotopy emerge in neonatal mice in the first week after birth, a period in which spontaneous retinal activity is mediated by nicotinic acetylcholine receptors containing the β2 subunit (β2-nAChRs; Feller et al., 1996; Bansal et al., 2000). Genetic and pharmacologic manipulations that impair β2-nAChR-mediated retinal waves cause deficits in visual system development, including defects in retinotopy and eye segregation (Stellwagen and Shatz, 2002; Chandrasekaran et al., 2005; Mrsic-Flogel et al., 2005; Rossi et al., 2001; Grubb et al., 2003; McLaughlin et al., 2003; Penn et al., 1998; Pfeiffenberger et al., 2005, 2006; Cang et al., 2005; Rebsam et al., 2009; Wang et al., 2009). However, these manipulations invariably change retinal activity levels in addition to disrupting retinal waves, making it ambiguous whether a threshold level of activity or specific patterns of spontaneous waves are important in map development. Moreover, genetic manipulations of spontaneous retinal waves have mainly utilized whole-animal knockouts (β2(KO) mice), leading to uncertainty about the retinal origin of the observed visual map phenotypes because of the broad expression of β2-nAChRs in the eye and brain.

Here, we establish an instructive role for spontaneous activity in neural circuit development by investigating the emergence of retinotopy and eye-specific segregation in a line of transgenic mice (β2(TG) mice) with β2-nAChR expression that is limited to the ganglion cell layer of the retina. A detailed examination of spontaneous activity in β2(TG) mice shows that a wide range of single-neuron RGC activity parameters are normal, but the spatiotemporal pattern (spread) of retinal waves is visibly truncated. Remarkably, this retinal wave manipulation completely disrupts the segregation of eye-specific inputs to the dLGN and SC but has no influence on the development of retinotopic maps in the monocular zone of the dLGN and SC. These results demonstrate that the presence of normal levels of spontaneous retinal activity, including bursts of spikes and even "small" retinal waves, is not sufficient to produce normal circuits. Rather, we identify specific spatiotemporal patterns of spontaneous retinal activity that are necessary for the emergence of eye-specific segregation, and distinct aspects of retinal activity that mediate the development of retinotopy. This shows that spontaneous retinal waves are not just permissive but instructive in the development of the visual system and suggests that specific and distinct patterns of spontaneous activity found throughout the developing brain are essential in the emergence of specific and distinct patterns of neuronal connectivity.

RESULTS

Inducible Expression of β2-nAChRs in the Retina

We examined the role of retinal β2-nAChRs and spontaneous waves in visual map development utilizing a line of transgenic mice with retina-specific expression of β2-nAChRs. Retinal specificity is achieved in these transgenic mice, referred to here as β2(TG) mice, by expressing the tetracycline transactivator under control of the neuron-specific enolase promoter (*NSE-tTA*) and β2-nAChRs under the control of a tetracycline-regulated promoter (*TetOp-β2*) on a β2-null background (Figures 1A and 1B; King et al., 2003). In this system (Shockett et al., 1995), in the absence of tetracycline, *tTA* binds to a promoter consisting of the tetracycline operator (*TetOp*) to drive the expression of β2-nAChRs. When tetracycline is present, *tTA* undergoes a conformational change that interferes with binding to the *TetOp* promoter, and the transcription of β2-nAChRs is inhibited. Retina specific expression of β2-nAChRs in the β2(TG) mice was confirmed using [^{125}I]A85380, a specific ligand for nicotinic receptors containing the β2 subunit (Mukhin et al., 2000). In WT mice (Figure 1B), [^{125}I]A85380 binding is found throughout the brain but is absent in β2(KO) mice. In β2(TG) mice, [^{125}I]A85380 is found only in retino-recipient targets such as the dLGN and SC. This label is eliminated when both eyes are enucleated, confirming the retina-specific expression of β2-nAChRs in β2(TG) mice. Within the retina, expression of β2-nAChR mRNA at P4 normally spans all retinal lamina (Figure 1C, top), but is strongest in the ganglion cell layer (GCL) and inner nuclear layer (INL) (Moretti et al., 2004). In β2(TG) mice, expression of β2-nAChR mRNA is largely absent from the INL, and is restricted to the GCL (Figure 1C, bottom).

Normal Single-Neuron Firing but Altered Retinal Waves in β2(TG) Mice

Since cholinergic synapses between amacrine cells in the INL are thought to mediate wave propagation within the early neonatal retina (Blankenship and Feller, 2010) but are absent in β2(TG) mice, we used a multielectrode array in vitro to examine spontaneous RGC activity in β2(TG) and WT mice. We compared a wide range of RGC spontaneous activity properties, including firing rate (Figure 1E), the prevalence of bursts and percent of spikes in bursts (Figure 1F; Table 1). Normal levels of spontaneous retinal activity were observed in β2(TG) mice in comparison to WT mice (WT: 0.17 ± 0.12 Hz; β2(TG): 0.21 ± 0.08 Hz; mean ± SD, $p = 0.54$), and retinal expression of β2-nAChRs in β2(TG) mice was confirmed by the sensitivity of this spontaneous activity to the β2-nAChR-specific antagonist, Dihydro-beta-erythroidine (DHβE) (Figure 1E). In fact, all spontaneous activity properties for RGCs considered in isolation were similar in β2(TG) mice and WT mice, but the spatiotemporal properties of retinal waves were visibly abnormal (Figures 1D–1G; Table 1; see Movie S1 and Movie S2 available online). While waves are clear, consistent and just as frequent in the retina of β2(TG) mice as WT mice, they are much smaller in spatial extent than normal (Figures 1D and 1F), and activity correlations between RGCs fall off much more steeply with separation in comparison to WT mice (Figure 1G). Thus, β2(TG) mice are a suitable model system for distinguishing between a permissive role and an instructive role of spontaneous retinal activity in the development of maps for eye-specific segregation and retinotopy in the mouse.

Normal Retinotopy in the SC of β2(TG) Mice

First, we examined the impact of spatially restricted ("small") retinal waves on the development of retinotopy in the SC of β2(TG) mice. Dorsal RGCs in β2(TG) mice, which project only to the contralateral SC in mice (Dräger and Olsen, 1980), have retinotopic projections that are indistinguishable from WT mice (Figures 2A and 2B). The size of the RGC target zone in the SC of β2(TG) mice (1.08% ± 0.48%, mean ± SD) is no different than WT mice (1.05% ± 0.25%, mean ± SD; $p = 0.85$) and

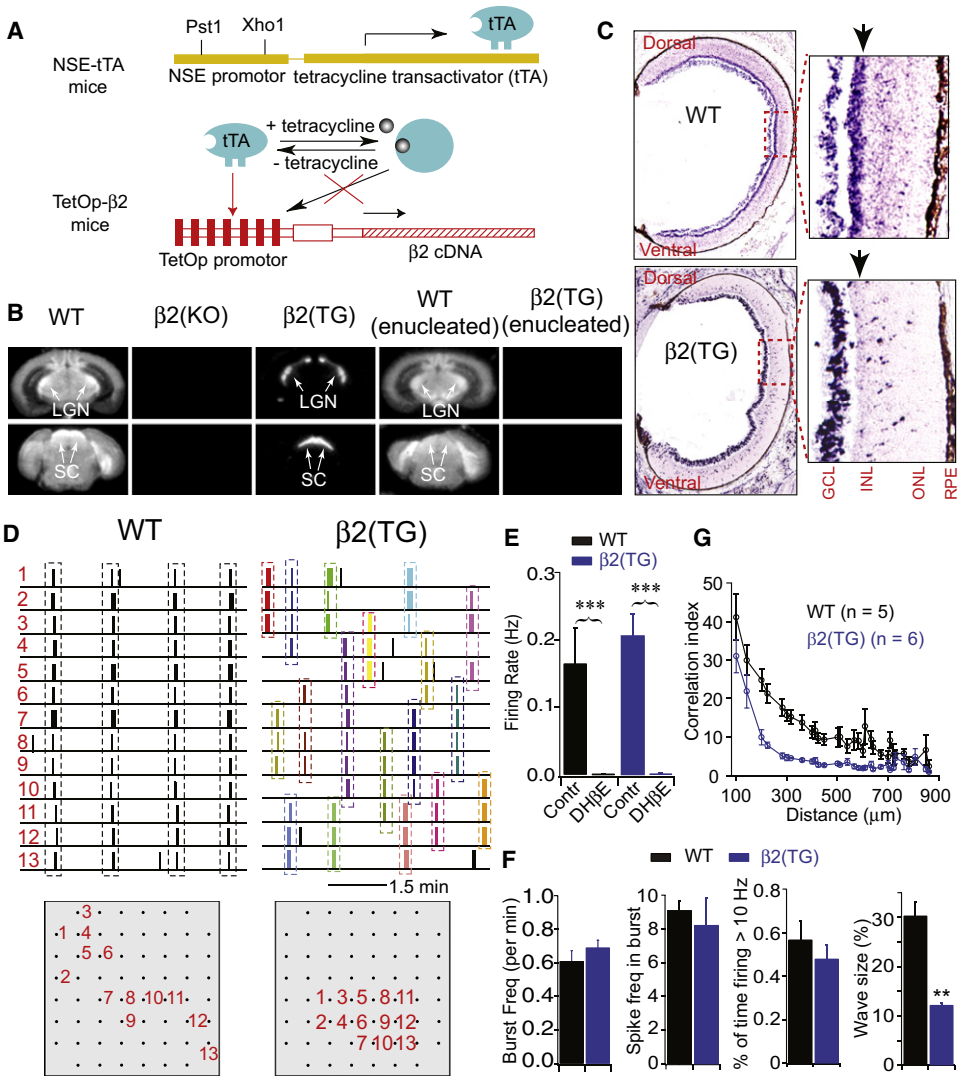

Figure 1. β2(TG) Mice Express β2-nAChRs Only in the Ganglion Cell Layer of the Retina, Have Normal RGC Firing Properties When Considered in Isolation, but Have Small Retinal Waves

(A) Expression of β2-nAChRs in the β2(TG) retina is controlled by a Tet-Off system, formed through the expression of both *NSE-tTA* and *TetOp-β2* transgenes.

(B) β2-nAChRs are broadly expressed in WT mice, with no [^{125}I]A85380 binding in β2(KO) mice. In β2(TG) mice, binding is detected only in the optic tract, dLGN and SC. Enucleating both eyes completely eliminates binding in β2(TG) mice, demonstrating that β2-nAChRs in β2(TG) mice are expressed on RGC axon terminals.

(C) In situ hybridization for β2-nAChR mRNA in P4 WT and β2(TG) mice. In WT mice, β2-nAChR mRNA expression is broad, but highest in the ganglion cell layer (GCL) and inner nuclear layer (INL, arrow in top panel). In β2(TG) mice, β2-nAChR mRNA expression is concentrated in the GCL and much weaker in other retinal layers (arrow in bottom panel).

(D) Spontaneous RGC activity in P4 retina recorded in Ringer's solution at 37°C. RGC activity is synchronous across the entire multielectrode recording array (shown in gray at bottom) in WT mice, while there are only local patches of synchronous activity in β2(TG) mice.

(E) Retinal ganglion cell firing rates in WT and β2(TG) mice are similar ($p = 0.51$, two-tailed Student's t test) and sensitive to the β2-nAChR antagonist, DHβE.

(F) A wide range of RGC firing parameters were compared between WT and β2(TG) mice under a range of conditions (see also Table 1 and Table S2). Illustrated here are four of these parameters, including burst frequency, spike frequency in a burst, and percent of time firing greater than 10 Hz. Only parameters related to the spatiotemporal pattern of the waves, not spiking properties (independent of waves), differed between WT and β2(TG) mice. By far the largest difference between WT and β2(TG) mice is wave size ($p < 0.002$, two-tailed Student's t test).

(G) Correlation index (cross correlation) of RGC activity is broad in WT mice, but falls off more steeply with separation in β2(TG) mice.

dLGN, lateral geniculate nucleus; SC, superior colliculus; ONL, outer nuclear layer; RPE, retinal pigment epithelium. Triasterisk, $p < 0.001$, two-tailed Student's t test. Error bars are SEM. See also Figures S3, S5, and S6, Table S2, Movie S1, and Movie S2.

much smaller than β2(KO) mice (3.78% ± 1.49%, mean ± SD; $p < 0.001$ for both comparisons). The development of retinotopically refined projections in β2(TG) mice is clearly the consequence of transgene expression, as application of the tetracycline analog doxycycline, which suppresses β2-nAChRs expression in our TetOp-β2(TG) mice (Figure 1A), results in retinal

Table 1. Properties of Spontaneous Retinal Activity in WT and β2(TG) Mice

	WT	β2(TG)
Total firing rate (Hz)	**0.17 ± 0.12**	**0.21 ± 0.08**
% of firing time > 10 Hz	**0.57 ± 0.19**	**0.48 ± 0.15**
Wave freq. (per min)	0.81 ± 0.09	0.74 ± 0.17
Wave duration (s)	1.78 ± 0.28	1.81 ± 0.49
Wave size (% of channels)	30.36 ± 6.05	12.21 ± 0.78**
Wave firing rate (Hz)	3.65 ± 0.38	3.90 ± 0.44
% spikes in waves	93.74 ± 1.75	83.79 ± 3.92
% bursts in waves	94.44 ± 3.45	77.67 ± 3.56***
Burst freq (per min)	**0.61 ± 0.14**	**0.69 ± 0.11**
% Spikes in bursts	**66.66 ± 10.60**	**73.15 ± 3.27**
Burst duration (s)	**2.37 ± 1.37**	**2.64 ± 1.03**
ISI in burst (s)	**0.54 ± 0.40**	**0.44 ± 0.19**
Spike freq. in burst	**9.11 ± 1.23**	**8.23 ± 3.53**
Interburst interval (s)	**112.69 ± 31.83**	**93.58 ± 18.35**

A wide range of spontaneous retinal activity parameters were quantified and compared in β2(TG) mice and WT mice. Nearly all of these parameters are comparable in β2(TG) and WT mice, with the conspicuous exception of retinal wave size (spatial extent), which is 3–5 times smaller in β2(TG) mice than WT mice. Spiking properties that are independent of waves (shown in bold), such as firing rate, burst frequency and ISI in bursts, are all comparable in β2(TG) and WT mice. Similar findings were observed when spontaneous retinal activity was examined in a variety of different recording media or at 31°C instead of 37°C (Table S2). Means ± SD are reported; **$p < 0.01$; ***$p < 0.001$.

projections that are as poorly refined as in β2(KO) mice (Figures 2A and 2B; 3.43% ± 1.92% with doxycycline, mean ± SD; $p = 0.002$ in comparison with β2(TG) and $p = 0.66$ in comparison with β2(KO)). This data demonstrates that small retinal waves and the expression of β2-nAChRs in the retina, and not the SC, are sufficient for the development of normal retinotopy in mice.

Impaired Eye-Specific Segregation in the SC of β2(TG) Mice

While RGC projections in mice are mostly crossed, about 5% of RGCs project ipsilaterally (Dräger and Olsen, 1980). Crossed projections in the SC form a retinotopic map and also segregate with respect to eye of origin, with a superficial layer (the SGS) in the SC that receives exclusive input from the contralateral eye, and a slightly deeper layer (the SO) that receives input from the ipsilateral eye (Figures 2C and 2D). Remarkably, eye segregation is profoundly disturbed in β2(TG) mice (fraction of SGS with ipsi: 3.17% ± 1.28%, mean ± SD for WT; 33.01% ± 9.06%, mean ± SD, for β2(TG); $p < 0.001$; % overlap: 2.63 ± 1.69, mean ± SD, for WT; 32.82 ± 9.06, mean ± SD, for β2(TG); $p < 0.001$), and eye-specific lamina remain as poorly formed in the SC of β2(TG) mice as in mice completely lacking β2-nAChRs (β2(KO) mice; fraction of SGS with ipsi: 37.31% ± 10.95%, mean ± SD, for β2(KO); % overlap: 37.19 ± 10.95, mean ± SD; $p = 0.2361$ and 0.2286 for comparison between β2(KO) and β2(TG)) (Figures 2C, 2D, and S1).

Normal Retinotopy Only in the Absence of Binocular Competition in the SC of β2(TG) Mice

Due to the lateral position of their eyes, binocular projections in mice are limited to RGCs from the extreme ventral-temporal retina (Dräger and Olsen, 1980; Godement et al., 1984). Curiously, retinotopic refinement in β2(TG) mice is normal in RGCs from throughout the retina with the exception of those from the ventral-temporal crescent (Figures 3A–3D and S2; Table S1); those RGC axons that fail to segregate with respect to eye of origin also lack retinotopic refinement. The failure of RGC axons from the binocular zone of the retina to refine in β2(TG) mice is not due to incomplete rescue of β2-nAChRs expression in ventral-temporal retina, as in situ hybridization shows that β2-nAChR mRNA levels are indistinguishable in dorsal and ventral retina (Figure 1C), and spontaneous retinal waves in ventral-temporal retina of β2(TG) mice are indistinguishable from dorsal-nasal retina (Figure S3). Furthermore, enucleating one eye at birth fully restores retinotopy of the ventral-temporal (binocular zone) RGC axons from the intact eye (Figures 3E and 3F; Table S1). This unambiguously demonstrates that "small" retinal waves even in ventral-temporal RGCs are completely capable of mediating retinotopic refinement, but RGC interactions between the two eyes impairs retinotopy in the binocular zone of the SC in β2(TG) mice.

Normal Retinotopy but Impaired Eye-Specific Segregation in the dLGN of β2(TG) Mice

The SC and the dLGN are the dominant targets of retinal projections in mammals. Despite its relatively small size in rodents, RGC projections to the dLGN are segregated with respect to eye of origin and display sharp retinotopic organization (Lund et al., 1974; Godement et al., 1984; Pfeiffenberger et al., 2006). We examined retinotopy and eye segregation in the dLGN of β2(TG) mice and observed conditions analogous to that in the SC. In particular, we found that the retinotopy of projections to the dLGN from the dorsal monocular zone of the retina are normal (Figures 4A and 4B; 12% ± 14%, mean ± SD for WT; 29% ± 11%, mean ± SD for β2(KO); 17% ± 9%, mean ± SD for β2(TG); $p < 0.001$ for comparison between β2(KO) and both WT and β2(TG)), but RGC projections from the ventral-temporal binocular zone of the retina remain unrefined (Figures 4C and 4D; 18% ± 5%, mean ± SD for WT; 40% ± 10%, mean ± SD for β2(KO); 41% ± 9%, mean ± SD for β2(TG); $p < 0.001$ for comparison between WT and both β2(KO) and β2(TG)), unless binocular competition is removed through monocular enucleation (Figures 4E, 4F, and S4; 22% ± 5%, mean ± SD for WT; 42% ± 8%, mean ± SD for β2(KO); 25% ± 8%, mean ± SD for β2(TG); $p < 0.001$ for comparison between β2(KO) and WT; $p = 0.005$ between β2(KO) and β2(TG); $p = 0.52$ for comparison between β2(TG) and WT). Eye-specific segregation is also completely disrupted in the dLGN of β2(TG) mice, like in β2(KO) mice (Figures 4G–4K; Rossi et al., 2001; Muir-Robinson et al., 2002; Grubb et al., 2003; Pfeiffenberger et al., 2005, 2006). These data demonstrate that normal levels of spontaneous neuronal activity and "small" retinal waves are not sufficient to mediate the segregation of retinal afferents with respect to eye of origin in the dLGN and SC but are sufficient to mediate normal retinotopy (in the absence of binocular competition) throughout the dLGN and SC.

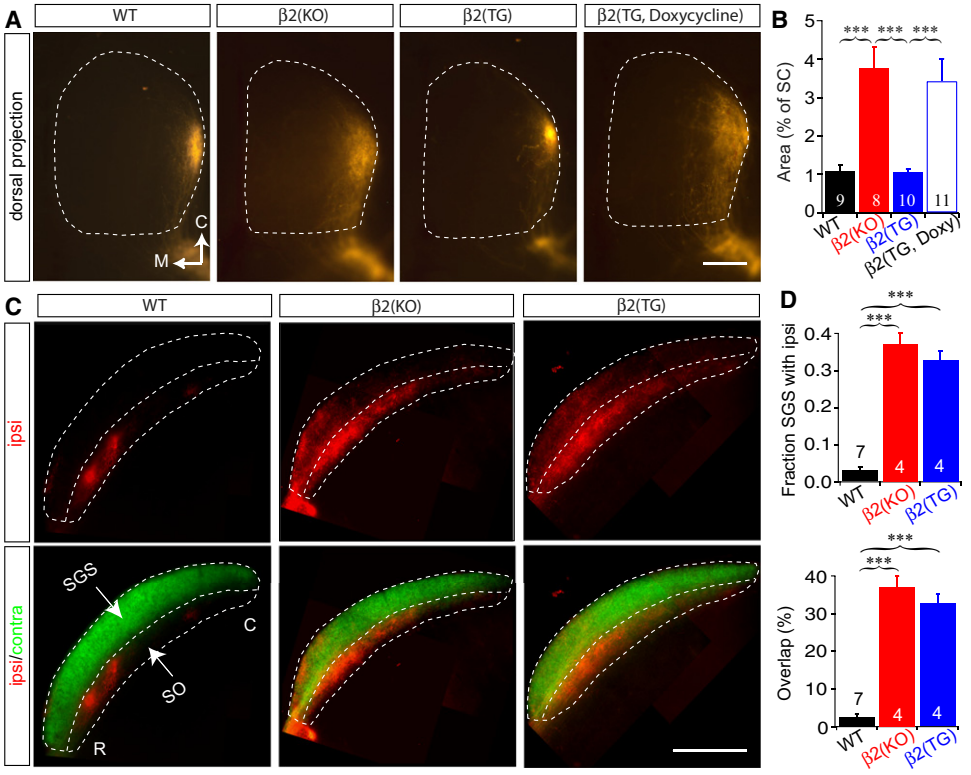

Figure 2. Retinotopic Map Refinement, but Not Eye-Specific Segregation, Is Rescued in the SC of β2(TG) Mice

(A and B) Focal DiI injections into dorsal retina result in a spot of label in the SC (whole-mount, dorsal view). The target zone spot in β2(KO) mice and β2(TG) mice treated with doxycycline is much larger than in WT and β2(TG) mice.

(C and D) Whole-eye (vitreal) injections of Alexa-conjugated cholera toxin dye bulk label most RGC axon projections in the SC. Contralateral axons are green, ipsilateral red. Contralateral axons (green) project to the most superficial (SGS) layer of the SC (sagittal sections), ipsilateral eye axons (red) project to the SO layer just inferior to the contralateral axons. A large fraction of axons from the ipsilateral eye extend into the SGS layer in both β2(KO) and β2(TG) mice (D, top) and overlap with projections from the contralateral eye (D, bottom), indicating poor eye segregation.

M, medial; C, caudal; R, rostral; SGS, stratum griseum superficial; SO, stratum opticum. Scale bars ,500 μm for all figures. Biasterisk, $p < 0.01$, and triasterisk, $p < 0.001$, two-tailed Student's t test. Error bars are SEM. See also Figures S1 and S8.

Chronic Binocular Application of CPT-cAMP Rescues Eye Segregation in β2(TG) Mice

We tested whether the abnormal spatiotemporal properties of waves in the β2(TG) mice are responsible for their visual map defects by manipulating β2(TG) retinal waves pharmacologically in vivo. Spontaneous retinal activity, retinal wave dynamics, and size are modulated by cAMP levels (Stellwagen and Shatz, 2002; Stellwagen et al., 1999; Zheng et al., 2006). Acute application of CPT-cAMP and other cAMP signaling agonists increases retinal wave size and frequency (Stellwagen and Shatz, 2002; Stellwagen et al., 1999). Daily binocular intravitreal injection of CPT-cAMP, a nonhydrolyzable membrane-permeable analog of cAMP, beginning at P2 in β2(TG) mice significantly improves eye-specific segregation in both the dLGN and SC in comparison to saline (control) injections (Figure 5). This strengthens the assertion that the altered spatiotemporal properties of retinal waves in β2(TG) mice are responsible for their visual map defects, and demonstrates that expression of β2-nAChRs in the dLGN and SC is not necessary for eye-specific RGC axon segregation.

Computational Model for the Role of Spatiotemporal Retinal Wave Patterns in Visual Map Development

We constructed a computational model using activity-dependent Hebbian rules for synapse development to examine whether the mapping phenotype in β2(TG) mice can be explained based purely on the altered spatial properties of their retinal waves (Figure 6). In the model (Figure 6A), retinocollicular synapses develop according to a Hebbian plasticity rule, and compete with each other through the homeostatic regulation of total synaptic input to each SC neuron (see Experimental Procedures for more computational model details). At the beginning of each simulation, RGC projections to the SC are broad, and the binocular SC receives mixed input from the two eyes. During the simulation, retinal activity gradually modifies the pattern of retinocollicular connectivity through Hebbian synaptic plasticity rules so that after each retinal wave some of the synapses are potentiated and others are weakened, depending on the size, position and eye of origin of the wave.

We simulated the difference in map development between WT and β2(TG) mice by varying the spatial extent of waves while

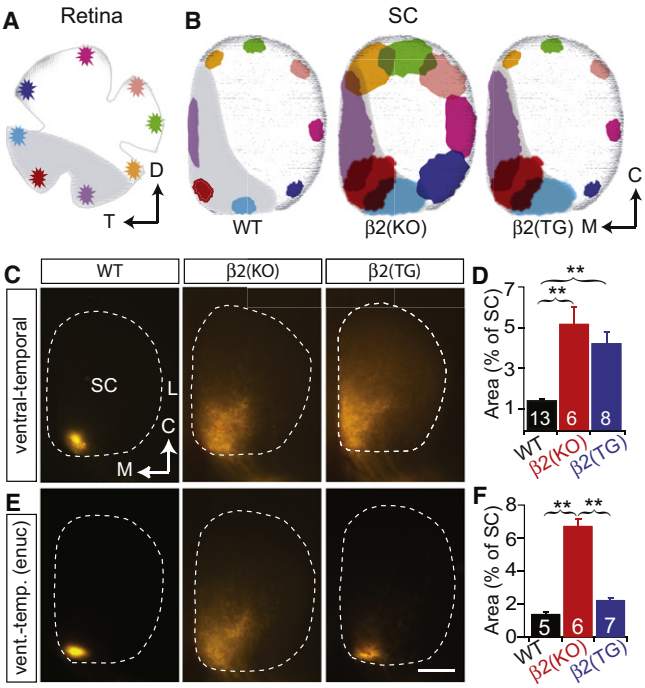

Figure 3. Binocular Competition Interferes with Retinotopic Map Refinement

(A and B) Focal DiI injections around the periphery of the retina results in focal target spots in the SC of WT mice, but much larger target zones in β2(KO) mice (see also Figure S2). In β2(TG) mice, target zones are completely restored in regions of the SC that receive monocular input but remain enlarged in the regions that receive input from both eyes (shown in gray).

(C and D) Focal DiI injections into ventral-temporal retina, which projects bilaterally, labels a spot in the rostromedial portion of the contralateral SC in WT mice. A similar injection in β2(KO) and β2(TG) mice results in a much larger target zone.

(E and F) Enucleation of one eye at birth restores retinotopic refinement of ventral-temporal RGCs in β2(TG) mice, but not in β2(KO) mice.

M, medial; C, caudal; T, temporal; D, dorsal. Biasterisk, $p < 0.01$, two-tailed Student's t test. Error bars are SEM. See also Table S1.

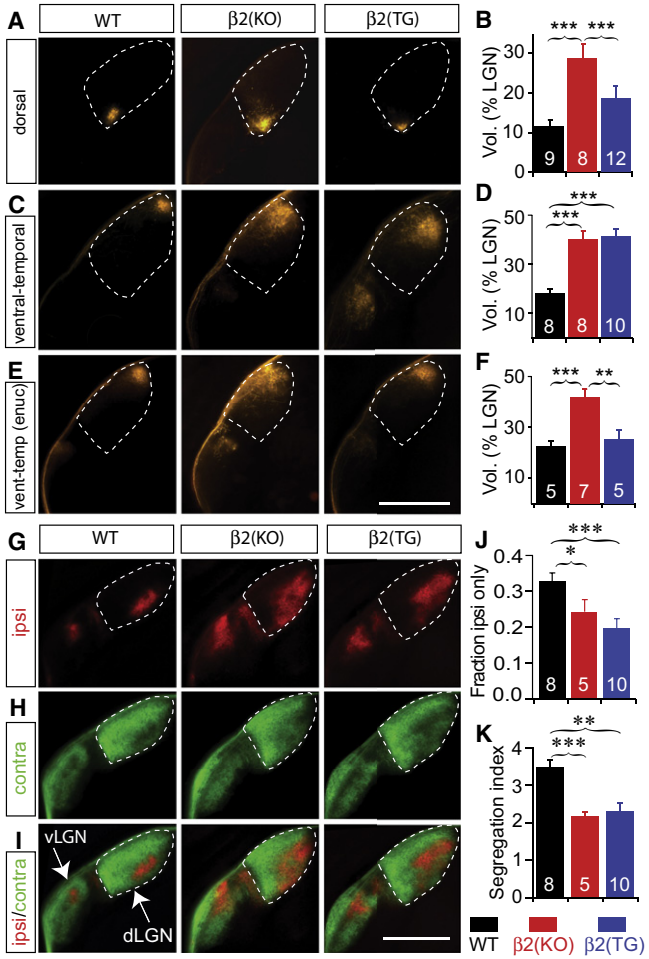

Figure 4. Retinotopic Map Refinement, but Not Eye-Specific Segregation, Is Rescued in the dLGN of β2(TG) Mice

(A and B) Focal DiI injections into dorsal retina result in a large spot of label in the dLGN (coronal sections) of β2(KO) mice, but small spots in WT and β2(TG) mice.

(C and D) Focal DiI injections into ventral-temporal retina labels a focal target spot in the contralateral dLGN of WT mice, but produces a much larger target zone in both β2(KO) and β2(TG) mice.

(E and F) Enucleation of one eye improves retinotopic refinement of ventral-temporal RGC axons in the dLGN of β2(TG) mice, but not β2(KO) mice.

(G–I) In the dLGN (coronal sections) of WT mice, RGC projections from the contralateral eye (green) are strictly excluded from the ipsilateral RGC axon terminal region (red). In β2(KO) and β2(TG) mice, ipsilateral eye projections have an expanded termination zone and intermingle with projections from the contralateral eye.

(J and K) Two measures of eye-specific segregation in the dLGN show that eye segregation is much better in WT mice (0.33 ± 0.07, mean ± SD for Fraction ipsi only; 3.42 ± 0.51, mean ± SD, for Segregation index) than β2(KO) mice (0.24 ± 0.08, mean ± SD, for Fraction ipsi only; 2.11 ± 0.25, mean ± SD for Segregation index) or β2(TG) mice (0.20 ± 0.08, mean ± SD, for Fraction ipsi only; 2.27 ± 0.78, mean ± SD, for Segregation index).

Biasterisk, $p < 0.01$, and triasterisk, $p < 0.001$, two-tailed Student's t test. Error bars are SEM. Scale bars, 500 μm for all figures. See also Figure S4.

maintaining the same level of overall retinal activity and the same frequency of waves per RGC, as observed experimentally. In simulations with large retinal waves (WT mice), inputs from the two eyes segregate so that neurons in the binocular SC become responsive to input from only one eye (Figure 6B). Large waves also induce retinotopic refinement of retinocollicular projections, both in the monocular and binocular SC, by strengthening retinotopically correct projections and weakening spatially inappropriate ones. Notably, simulations with small retinal waves reproduce both the monocular and binocular mapping phenotype of β2(TG) mice. In the monocular SC (or throughout the SC in one-eye enucleated animals), small-wave simulations result in retinotopic refinement, but in the binocular SC, both eye segregation and retinotopic refinement are impaired (Figures 6B–6E).

Why, according to the model, is retinal wave size (spatial extent) important for proper formation of both visual maps? In the binocular zone of the SC/dLGN, afferents from the two eyes compete with each other so that during each retinal wave, inputs from the corresponding eye are strengthened while inputs from the opposing eye are weakened. With small retinal waves, the amount of cooperative activity among RGCs from

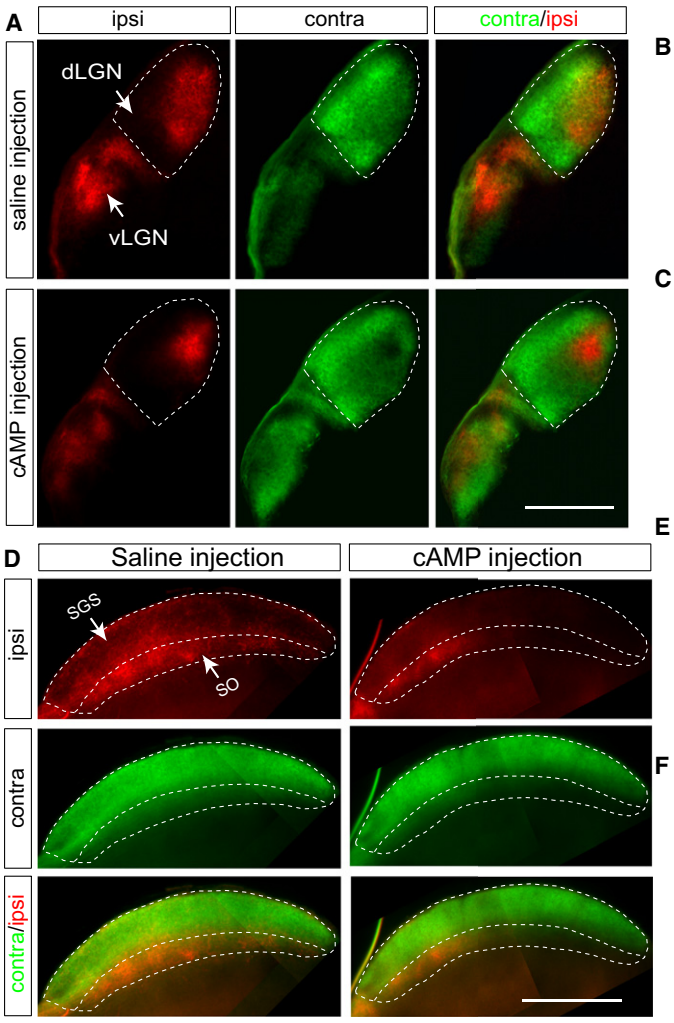

Figure 5. Daily Binocular Injections of CPT-cAMP Rescue Eye-Specific Segregation in β2(TG) Mice

(A) Example coronal sections show that binocular CPT-cAMP injections correct eye-specific segregation defects in the dLGN of β2(TG) mice compared to saline injection controls. Contralateral axons are labeled green, and ipsilateral axons are labeled red with whole eye (vitreal) injections of Alexa-conjugated cholera toxin.

(B) The fraction of dLGN with segregated ipsi projections is larger in CPT-cAMP-treated β2(TG) mice (0.31 ± 0.19, mean ± SD) than saline-treated β2(TG) mice (0.16 ± 0.12, mean ± SD, 10% threshold shown, difference was consistent across a range of thresholds).

(C) Eye-specific segregation in the dLGN measured with a segregation index was significantly improved in CPT-cAMP-treated β2(TG) mice (2.46 ± 0.31, mean ± SD) in comparison to that of saline-treated β2(TG) mice (1.70 ± 0.36, mean ± SD).

(D) Eye-specific segregation in the SC improves significantly in β2(TG) mice when treated with daily binocular injections of CPT-cAMP.

(E) Summary quantification of eye segregation measured as the fraction of the contralateral (SGS) layer with ipsi label (10% threshold shown, the difference was consistent across a range of thresholds). Fewer ipsilateral axons project to the contralateral (SGS) layer in CPT-cAMP-treated β2(TG) mice (22.43% ± 5.29%, mean ± SD) than in saline-treated β2(TG) mice (37.03% ± 2.32%, mean ± SD).

(F) Summary quantification of binocular overlap of ipsi (red) projections with contralateral (green) projections in the SGS layer. In CPT-cAMP-treated β2(TG) mice, the overlap was 22.15% ± 5.16% (mean ± SD). In saline-treated β2(TG) mice, the overlap was 35.95% ± 2.01% (mean ± SD). Triasterisk, $p < 0.001$, two-tailed Student's t test. Error bars are SEM.

one eye is correspondingly small, so the strengthening of a "waving" eye is greatly reduced compared to when the wave covers a large portion of the retina. Afferents from the two eyes still compete in the "small-wave" scenario, but competition in this case does a poor job distinguishing between afferents from the two eyes, resulting in degraded eye-specific segregation. The model also shows why impairing eye-specific segregation interferes with retinotopic refinement in the binocular zone of the SC/dLGN. Typically, as inputs from the two eyes segregate and strengthen, connections at retinotopically *inappropriate* locations are reduced through homeostatic regulation of the overall connectivity, but these spatially inappropriate connections *persist* in the absence of eye-specific segregation. If one eye is enucleated, interference from the other eye is eliminated, and small retinal waves are adequate to mediate retinotopic refinement even for ventral-temporal axons, as is normally the case in the monocular zone of the SC/dLGN. In sum, the model fully recapitulates the anatomical phenotypes observed in untreated and enucleated β2(TG) mice and demonstrates how specific spatiotemporal patterns of spontaneous retinal waves can dictate the emergence of specific patterns of neuronal connectivity during development.

DISCUSSION

There is a strong consensus in the field that during late stages of development (particularly in mammals), sensory driven neural activity profoundly shapes neural circuit structure and function. For instance, manipulating sensory experience (e.g., through monocular deprivation) produces dramatic shifts in neural response properties and corresponding changes in neural circuits during "critical periods" of development (Morishita and Hensch, 2008). It is also generally accepted that even during early stages of development, neurons need to be active for the brain to develop normally (Spitzer, 2006). However, it remains remarkably controversial whether this early neuronal activity acts in a passive way by triggering downstream cellular signaling pathways to promote cell survival and neurite outgrowth (potentially

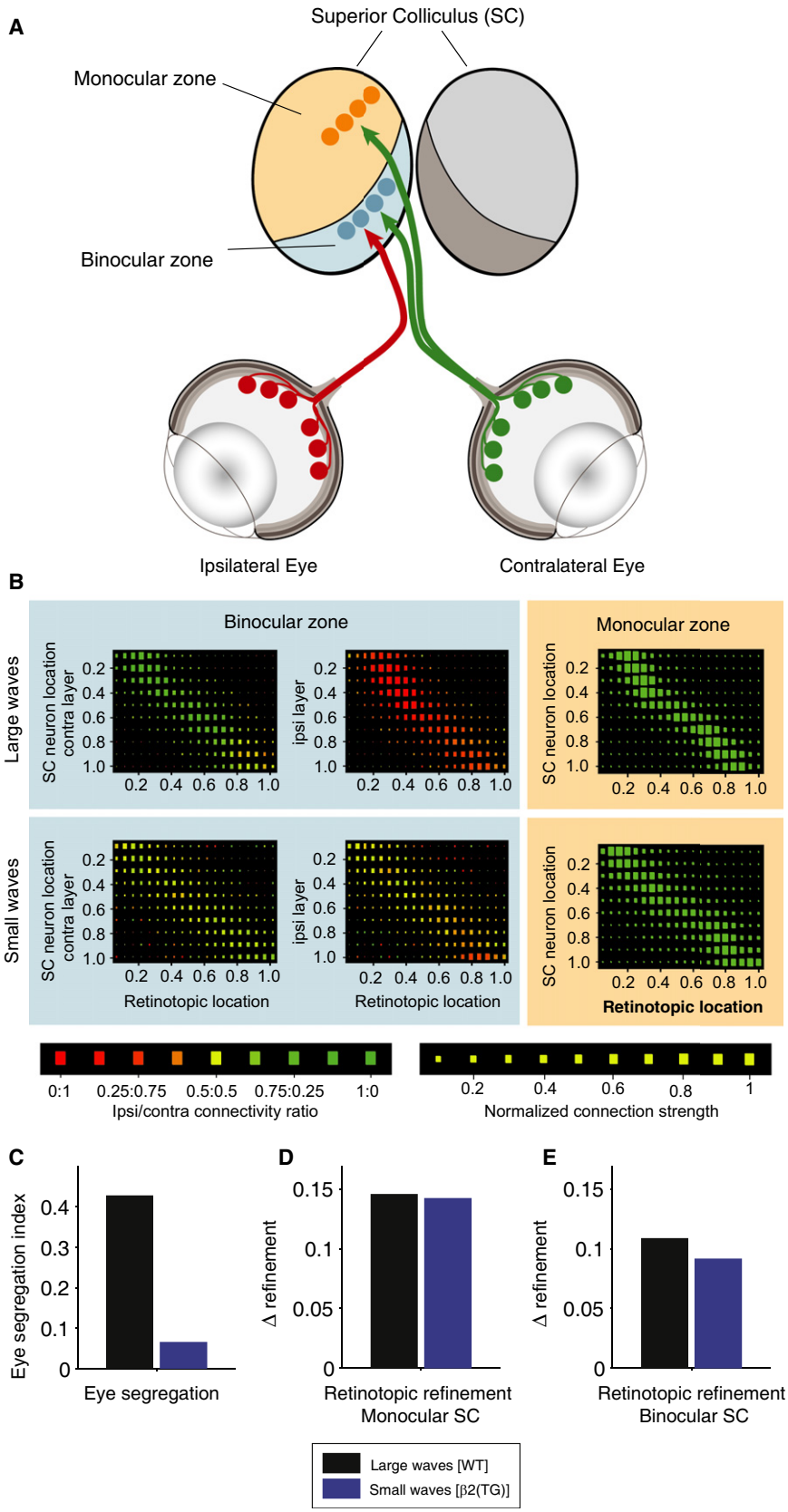

Figure 6. A Hebbian Model of Visual Map Development Recapitulates the Anatomical Phenotype Observed in β2(TG) Mice

(A) Schematic of the computational model. RGCs and SC neurons are represented by a one-dimensional array of spatially arranged computational units, and retinocollicular synaptic weights develop according to a standard Hebbian rule.

(B) Each row in the diagrams displays the afferent connectivity to one SC neuron at the end of a simulation. The size of the boxes indicates the strength of the corresponding synaptic connections, while their color indicates ocularity (red ipsilateral and green contralateral; see scales at bottom). Large retinal waves result in both eye-specific segregation (red or green, not yellow) and refinement of axonal arbors (narrow diagonal bands). Small waves, in contrast, generate robust retinotopic refinement in the monocular zone but result in dramatically impaired eye segregation as well as poor retinotopic refinement in the binocular zone (yellow and broad connectivity patterns).

(C–E) Quantification of simulation results for eye-specific segregation in the binocular SC and retinotopic refinement in the monocular and binocular SC. (C) Eye segregation is dramatically degraded by small waves in these simulations. (D) Retinotopic refinement is comparable for small and large waves in the monocular SC. (E) Retinotopic refinement is worse for small waves than large waves in the binocular SC. Eye segregation and retinotopic-refinement indices were averaged over SC neurons.

See also Figure S7.

through Ca^{2+} signaling) or in an instructive way, guiding neural circuit formation through specific spatiotemporal patterns of neural activity (Crair, 1999; Crowley and Katz, 2000; Huberman et al., 2008; Chalupa 2009; Feller, 2009). Patterns of spontaneous neuronal activity ("waves") have been described in a wide range of brain structures during early development, including the retina, thalamus, cortex, hippocampus, striatum, and spinal cord (Feller, 1999). Still, nowhere has it been established whether this patterned spontaneous activity is "permissive" or "instructive" in guiding brain development. Why has this fundamental question been so hard to nail down? Simply put, manipulations that change the spatiotemporal pattern of spontaneous neuronal activity have invariably also altered the activity of individual neurons (their overall spike rate or burst frequency, etc.). This completely confounds changes in interneuronal activity patterns with changes in single neuron activity levels. As a result this fundamental question, which permeates across a broad area of developmental neurobiology, remains unanswered.

Not Simply the Presence, But the Pattern of Retinal Waves Directs Visual Map Development

We demonstrated here that *patterns* of spontaneous neuronal activity *instruct* neural circuit development. We accomplished this with a novel line of transgenic mice (β2(TG)) in which we manipulated the expression of acetylcholine receptors responsible for the propagation of spontaneous waves in the inner retina. This genetic manipulation dramatically changed the spatiotemporal properties of spontaneous retinal waves (they become spatially restricted or "small") but had no effect on spiking properties of retinal ganglion cells when considered in isolation (wave properties change, but the spiking properties of individual retinal ganglion cells are unchanged). This "small wave" manipulation strikingly impaired the neural circuit that emerged between the retina and brain during development. This shows that not merely the presence, but the precise spatiotemporal pattern of spontaneous retinal activity instructs neural circuit development. These data are consistent with a body of literature arguing for an important role of activity-dependent competitive processes in mammalian brain development (Torborg et al., 2005; Chandrasekaran et al., 2005; Mrsic-Flogel et al., 2005; Penn et al., 1998; Cang et al., 2005; Katz and Shatz, 1996; Stryker and Harris, 1986; Cao et al., 2007) and demonstrate how even prior to sensory experience, patterned neuronal activity shapes developing brain circuits.

Retinotopic Refinement and Eye-Specific Segregation Rely on Different Aspects of Spontaneous Retinal Activity

β2(TG) mice have normal retinotopy but profoundly disturbed eye-specific segregation. To our knowledge, this is the first example of a distinction between the activity-dependent requirements for the development of these two visual maps and may reflect a fundamental difference between the process of retinotopic refinement and eye-specific segregation. Eye-specific segregation involves expulsion of "wrong-eye" axons from the domain of the "correct-eye." In an activity-dependent model, this process requires sufficient correlated intra-eye activity. Retinotopic refinement, in contrast, involves *relative* spatial correlations within an eye, where the activity of neighboring RGCs is more correlated than that of distant ones. Small retinal waves provide just these local correlations and are therefore adequate for mediating retinotopic refinement in the absence of binocular competition. This interpretation is further supported by our computational model for retinotopy and eye segregation, which is based on axonal competition and a Hebbian, correlation-based synaptic plasticity rule. This model produces both eye-specific segregation and retinotopy for a wide range of parameters only if the waves are sufficiently large, but only retinotopy if the waves are spatially small.

Binocular Interactions Can Interfere with Retinotopic Refinement

In β2(TG) mice, retinotopic refinement is normal everywhere except for the binocular zone of the dLGN and SC. Why? We believe the reason is an interference effect between RGC axons from the two eyes caused by the persistent defects in eye-specific segregation. We demonstrated that the expression of β2-nAChR mRNA is similar in ventral-temporal (binocular projecting) and dorsal-nasal (monocular) retina of β2(TG) mice. Retinal waves are also similar in ventral-temporal and dorsal-nasal retina of WT mice and β2(TG) mice. This argues strongly that intrinsic differences in β2-nAChR expression or retinal waves across the retina are not responsible for the selective retinotopic refinement failure of binocular zone RGC axons in β2(TG) mice. Moreover, enucleation of one eye completely restores retinotopic refinement of ventral-temporal RGC axons from the remaining eye, clearly demonstrating that ventral-temporal RGC axons are fully capable of normal retinotopic refinement in β2(TG) mice, but binocular interactions prevent this refinement. Analogous results have been reported in the ferret (Huberman et al., 2006), where binocular pharmacological blockade of retinal waves with epibatidine significantly enlarged the receptive fields of neurons with binocular receptive fields in the visual cortex but had no effect on the receptive fields of monocular neurons. These somewhat surprising results suggest that maps for retinotopy and eye-specific segregation are fundamentally linked; conditions that are appropriate for normal retinotopic refinement in the monocular zone may be inadequate to mediate retinotopic refinement in the presence of binocular competition. In the visual cortex, the plasticity of ocular dominance maps following monocular deprivation is linked to maps for stimulus orientation (Crair et al., 1997), but the current work specifically implicates the structure of spontaneous neuronal activity, not visual experience, in linking maps for retinotopy and eye of origin. Our Hebbian computational model recapitulates the link between eye-specific segregation and retinotopy. In simulations where binocular interactions persist due to poor eye segregation, retinotopic refinement is impaired as well. According to the model, if inputs from the two eyes do not segregate, the pattern of input activity to the SC and dLGN is fundamentally altered because it reflects activity from both eyes instead of one eye only. Normally, homeostatic regulation of the total synaptic input to neurons in the SC or dLGN favors the strengthening of highly correlated inputs from neighboring RGCs. However, the persistence of conflicting inputs from the two eyes interferes with the process of RGC axon pruning from

inappropriate retinotopic locations, and retinotopic refinement is impaired. By contrast, retinotopy develops normally in the monocular zone of β2(TG) mice and throughout the SC in enucleated β2(TG) mice, because conflicting signals from the two eyes do not exist under these conditions.

Why Are Retinal Waves Small in β2(TG) Mice?

β2-nAChRs are normally expressed throughout the developing retina (Moretti et al., 2004; Figure 1C), particularly in synapses among amacrine cells and between amacrine cells and ganglion cells (Blankenship and Feller, 2010). Retinal waves are thought to be nucleated by ChAT-positive intrinsically bursting starburst amacrine cells, and wave propagation across the retina mediated by β2-nAChR containing synapses between amacrine cells in the inner nuclear layer (Butts et al., 1999; Zheng et al., 2006). RGC firing during a wave is coupled to starburst amacrine cell bursting through synapses containing β2-nAChRs (Blankenship and Feller, 2010). However, little is known experimentally about specific mechanisms that regulate wave size. We reason that waves are small in the β2(TG) mice because β2-nAChR expression is largely limited to RGCs, which synaptically isolates starburst amacrine cells from each other and chokes off wave propagation across the inner retina. Since synaptic communication between amacrine cells in the inner nuclear layer and RGCs in the ganglion cell layer is preserved, RGCs in β2(TG) mice will faithfully relay the intrinsic bursting activity of underlying starburst amacrine cells, preserving overall activity levels but without the spatial spread typical of normal retinal waves. These data suggest that β2-nAChR expression is tightly regulated in the developing retina in order to promote the propagation of spontaneous waves with the appropriate spatiotemporal patterns that will drive eye segregation and retinotopic refinement.

What about β2(KO) Mice?

β2(KO) mice lack β2-nAChR expression throughout the brain and body, and both eye-specific segregation and retinotopic refinement are disturbed in the dLGN and SC (Rossi et al., 2001; Grubb et al., 2003; McLaughlin et al., 2003; Chandrasekaran et al., 2005). It is unlikely that these visual map deficits are due to the absence of β2-nAChR expression in the dLGN and SC because β2(TG) mice also lack expression in these RGC targets but retinotopy is normal in β2(TG) mice and eye-specific segregation can be rescued through the daily binocular application of CPT-cAMP. This demonstrates β2-nAChR expression in the dLGN and SC is not necessary for the development of retinotopy and eye-specific segregation in mice.

If β2-nAChR expression in the SC and dLGN is not required for retinotopic refinement or eye-specific segregation, why are visual maps disturbed in β2(KO) mice? Is it because waves are absent in β2(KO) mice, or very abnormal, or something else entirely? The precise effects of completely knocking out β2-nAChRs on retinal activity are controversial (Bansal et al., 2000; Sun et al., 2008; Stafford et al., 2009). Spontaneous retinal activity in β2(KO) mice is very sensitive to the precise in vitro recording conditions used to examine activity (Bansal et al., 2000; Sun et al., 2008; Stafford et al., 2009). Variations in temperature, composition of the recording medium or even ambient light levels (Figure S5; data not shown) can dramatically affect whether waves are even present in β2(KO) mice. In contrast, retinal waves in WT and β2(TG) mice are very stable and quite insensitive to these variations (Figure S6; Table S2). In particular, retinal wave size is consistently much smaller in β2(TG) mice relative to WT mice across all recording conditions, while other spontaneous retinal activity parameters are similar (Figure S6; Table S2), reinforcing the conclusion that visual map defects in β2(TG) mice are the result of altered retinal waves. Ultimately, it will be necessary to examine retinal wave properties in vivo in awake mice to determine definitively what specific aspects of spontaneous retinal activity are disturbed in β2(KO) mice that may lead to their disturbed visual maps. Regardless, spontaneous retinal activity in β2(KO) mice is abnormal under all reported conditions (Bansal et al., 2000; Sun et al., 2008; Stafford et al., 2009), and in the interim we propose that even if waves are present in vivo in β2(KO) mice, the majority of RGC activity is likely to reside outside of waves (Stafford et al. [2009] observed only ~30% of RGC activity resided in retinal waves, whereas >80% of activity is in waves in β2(TG) and WT mice [Table 1]). In this case, our computational model predicts that retinal activity will fail to induce either eye segregation or retinotopic map refinement in β2(KO) mice (Figure S6).

Sperry and Hebb in Visual Map Development

We have presented compelling evidence that the development of visual maps in the dLGN and SC is dependent not simply on the presence, but the precise pattern of spontaneous ongoing activity in the retina. What are the mechanisms that mediate this activity-dependent development at retinofugal synapses? Hebbian synaptic plasticity is known to exist at retinal ganglion cell synapses onto neurons in the dLGN (Butts et al., 2007) and SC (Shah and Crair, 2008). Furthermore, our computational model, based on a synaptic learning rule that obeys Hebbs postulate, fully captures the experimental results observed in β2(TG) mice. Of course, this does not exclude an essential role for molecular targeting events in visual map development. We (Chandrasekaran et al., 2005) and many others (e.g., Goodman and Shatz, 1993; Cline, 2003; Feller, 2009) have long argued that both molecular patterning events and activity-dependent mechanisms work together to wire the vertebrate visual system. It is possible that a molecular process that is *dependent* on the pattern of spontaneous neuronal activity but *independent* of synaptic plasticity (Hebb) or even synaptic function is responsible for the refined development of visual maps in the dLGN and SC. For example, specific neural activity patterns in RGCs may drive distinct patterns of cAMP oscillations and associated second messenger cascades, which then regulate neurite outgrowth and development to achieve map refinement (Kumada et al., 2009; Shelly et al., 2010; Nicol et al., 2007; Carrillo et al., 2010). In this case, our data show that the precise spatiotemporal pattern of spontaneous retinal waves is *still critical* for normal map development, but the result may be achieved through as-yet-unknown molecular mechanisms that are dependent on patterned neuronal activity but don't critically rely on synaptic function or Hebbian mechanisms at the synapse.

With the increasing power and ease of molecular-genetic techniques to identify molecules and genes involved in visual system development, it is tempting to focus on these signaling

pathways at the exclusion of more "traditional" activity-dependent processes. However, it seems clear that both molecules and activity play important roles in visual map development, and the expression of genes involved in visual system development is likely tightly regulated by activity-dependent processes and vice-versa. Indeed, several molecules and signaling pathways recently shown to be involved in visual map development were initially identified through differential screens for genes regulated by neuronal activity (e.g., Shatz, 2009). The results described here show that even rather subtle genetic manipulations that only alter patterns of spontaneous activity without changing the levels of activity can have a profound impact on brain development. This may have significant implications for diseases of multigenetic origin, such as schizophrenia and autism, in which brain wiring may be negatively affected not because of direct effects of genes on neural circuits or synaptic function, but because of indirect effects on patterns of spontaneous or evoked activity during neural circuit development.

EXPERIMENTAL PROCEDURES

Animals

β2-nAChR subunit knockout β2(KO) and transgenic β2(TG) mice with retina-specific expression of β2-nAChRs were generated as described (King et al., 2003). Wild-type (WT) mice (C57BL/6J) were obtained from Jackson Laboratory (Bar Harbor, ME). Doxycycline administration was provided through the mothers of experimental mice via water containing doxycycline (1mg/ml) from E0 to P8. Animals were treated in compliance with the Yale IACUC, U.S. Department of Health and Human Services, and Institution guidelines.

Eye Injections, Fluorescent Images, and Data Analysis

Focal DiI injections (2.3 nl) for measurements of retinotopy were performed, imaged and quantified blind to genotype as described (Chandrasekaran et al., 2005). Injections were localized along the perimeter of the retina, using as a reference the insertion points of the four major eye muscles (Plas et al., 2005). Retinal injection size, quantified by measuring the area of fluorescent signal in the retina above one-half of the maximum fluorescent signal after background subtraction, showed no difference across all genotypes and injection locations, and there was no relationship between TZ area and retinal injection area (Figure S7; McLaughlin et al., 2003).

Measurements of eye-specific segregation were performed with whole eye injections (1 μl into the vitreous) of Alexa Fluor 488-conjugated cholera toxin (left eye) and Alexa Fluor 594 (right eye) at P6, then returned to their mother for 24–48 hr to allow transport of tracer from the retina to the SC and dLGN. CPT-cAMP treated animals were injected daily with 500 nl of saline or CPT-cAMP (5 mM) into both eyes from P2 to P6, then received whole eye injections of Alexa dye at P7. Eye-specific segregation in the SC was quantified by measuring the fraction of fluorescence signal labeled from the ipsilateral eye in the SGS layer, and also by measuring the overlap (in % of pixels) of ipsilateral eye fluorescence signal with contralateral eye fluorescence signal in the SGS layer. Quantification of eye-specific segregation in the dLGN followed previously published methods (Stellwagen and Shatz, 2002; Huberman et al., 2003; Torborg et al., 2005).

[^{125}I]A85380 Binding Assay

The [^{125}I]A85380 binding assay was performed on 15 μm brain sections as previously described (King et al., 2003).

In Situ Hybridization

Expression patterns were determined by means of non-radioactive in situ hybridization (ISH) on frozen sagittal sections of P4 mouse brains by the in situ hybridization core at Baylor College of Medicine following published methods (Visel et al., 2004).

Retinal Wave Recording and Data Analysis

Spontaneous RGC activity was recorded at P4 using a multielectrode array at 37°C in Ringer's solution (unless otherwise noted) following previously published protocols (Tian and Copenhagen, 2003; Xu et al., 2010). Various retinal wave properties were measured, including firing rate, correlation index, wave frequency, wave size, burst frequency, and burst duration. Wave size was defined as the fraction of all electrodes that were capable of recording spikes from at least one cell with a firing rate not less than 2 Hz during a wave. The correlation index was calculated as previously described (Torborg and Feller, 2004). Burst analysis was carried out using the burst analysis algorithm provided by Neuroexplorer (Nex Technologies, Lexington, MA) following previous published protocols (Sun et al., 2008; Stafford et al., 2009).

Computational Model

We constructed a computational model of retinocollicular map development in which RGC projections to SC neurons develop through a Hebbian plasticity rule. The model simulates the essential aspects of retinocollicular circuitry while retaining a level of simplicity that generalizes across biological details but allows for examination of the consequences of varying retinal wave size on visual map development. The difference in map development between WT and β2(TG) mice is modeled by modifying the spatial extent and frequency of waves, keeping constant the overall level of retinal activity per RGC, as observed experimentally.

SUPPLEMENTAL INFORMATION

Supplemental Information includes eight figures, two movies, and Supplemental Experimental Procedures and can be found with this article online at doi:10.1016/j.neuron.2011.04.028.

ACKNOWLEDGMENTS

We would like to thank members of the Crair lab for valuable comments on the manuscript, particularly Onkar Dhande and James Ackman, and Yueyi Zhang for technical help. This work was supported by NIH grant P30 EY000785 to M.C.C., D.Z., N.T., and Z.J.Z.; R01 EY015788 to M.C.C.; R01 EY012345 to N.T.; R01 EY014990 to D.Z.; R01 EY010894 and EY017353 to Z.J.Z.; an RPB Challenge Grant to the Department of Ophthalmology and Visual Science and R01 DA14241 and DA10455 to M.R.P. M.C.C. also thanks the family of William Ziegler III for their support.

Accepted: April 5, 2011
Published: June 22, 2011

REFERENCES

Bansal, A., Singer, J.H., Hwang, B.J., Xu, W., Beaudet, A., and Feller, M.B. (2000). Mice lacking specific nicotinic acetylcholine receptor subunits exhibit dramatically altered spontaneous activity patterns and reveal a limited role for retinal waves in forming ON and OFF circuits in the inner retina. J. Neurosci. *20*, 7672–7681.

Bekoff, A., Stein, P.S., and Hamburger, V. (1975). Coordinated motor output in the hindlimb of the 7-day chick embryo. Proc. Natl. Acad. Sci. USA *72*, 1245–1248.

Blankenship, A.G., and Feller, M.B. (2010). Mechanisms underlying spontaneous patterned activity in developing neural circuits. Nat. Rev. Neurosci. *11*, 18–29.

Butts, D.A., Feller, M.B., Shatz, C.J., and Rokhsar, D.S. (1999). Retinal waves are governed by collective network properties. J. Neurosci. *19*, 3580–3593.

Butts, D.A., Kanold, P.O., and Shatz, C.J. (2007). A burst-based "Hebbian" learning rule at retinogeniculate synapses links retinal waves to activity-dependent refinement. PLoS Biol. *5*, e61. 10.1371/journal.pbio.0050061.

Cang, J., Rentería, R.C., Kaneko, M., Liu, X., Copenhagen, D.R., and Stryker, M.P. (2005). Development of precise maps in visual cortex requires patterned spontaneous activity in the retina. Neuron *48*, 797–809.

Cao, L., Dhilla, A., Mukai, J., Blazeski, R., Lodovichi, C., Mason, C.A., and Gogos, J.A. (2007). Genetic modulation of BDNF signaling affects the outcome of axonal competition in vivo. Curr. Biol. *17*, 911–921.

Carrillo, R.A., Olsen, D.P., Yoon, K.S., and Keshishian, H. (2010). Presynaptic activity and CaMKII modulate retrograde semaphorin signaling and synaptic refinement. Neuron *68*, 32–44.

Chalupa, L.M. (2009). Retinal waves are unlikely to instruct the formation of eye-specific retinogeniculate projections. Neural Dev. *4*, 25.

Chandrasekaran, A.R., Plas, D.T., Gonzalez, E., and Crair, M.C. (2005). Evidence for an instructive role of retinal activity in retinotopic map refinement in the superior colliculus of the mouse. J. Neurosci. *25*, 6929–6938.

Cline, H. (2003). Sperry and Hebb: oil and vinegar? Trends Neurosci. *26*, 655–661.

Crair, M.C. (1999). Neuronal activity during development: permissive or instructive? Curr. Opin. Neurobiol. *9*, 88–93.

Crair, M.C., Ruthazer, E.S., Gillespie, D.C., and Stryker, M.P. (1997). Relationship between the ocular dominance and orientation maps in visual cortex of monocularly deprived cats. Neuron *19*, 307–318.

Crowley, J.C., and Katz, L.C. (2000). Early development of ocular dominance columns. Science *290*, 1321–1324.

Dräger, U.C., and Olsen, J.F. (1980). Origins of crossed and uncrossed retinal projections in pigmented and albino mice. J. Comp. Neurol. *191*, 383–412.

Feller, M.B. (1999). Spontaneous correlated activity in developing neural circuits. Neuron *22*, 653–656.

Feller, M.B. (2009). Retinal waves are likely to instruct the formation of eye-specific retinogeniculate projections. Neural Dev. *4*, 24.

Feller, M.B., Wellis, D.P., Stellwagen, D., Werblin, F.S., and Shatz, C.J. (1996). Requirement for cholinergic synaptic transmission in the propagation of spontaneous retinal waves. Science *272*, 1182–1187.

Godement, P., Salaün, J., and Imbert, M. (1984). Prenatal and postnatal development of retinogeniculate and retinocollicular projections in the mouse. J. Comp. Neurol. *230*, 552–575.

Goodman, C.S., and Shatz, C.J. (1993). Developmental mechanisms that generate precise patterns of neuronal connectivity. Cell. Suppl. *72*, 77–98.

Grubb, M.S., Rossi, F.M., Changeux, J.P., and Thompson, I.D. (2003). Abnormal functional organization in the dorsal lateral geniculate nucleus of mice lacking the beta 2 subunit of the nicotinic acetylcholine receptor. Neuron *40*, 1161–1172.

Huberman, A.D., Wang, G.Y., Liets, L.C., Collins, O.A., Chapman, B., and Chalupa, L.M. (2003). Eye-specific retinogeniculate segregation independent of normal neuronal activity. Science *300*, 994–998.

Huberman, A.D., Speer, C.M., and Chapman, B. (2006). Spontaneous retinal activity mediates development of ocular dominance columns and binocular receptive fields in v1. Neuron *52*, 247–254.

Huberman, A.D., Feller, M.B., and Chapman, B. (2008). Mechanisms underlying development of visual maps and receptive fields. Annu. Rev. Neurosci. *31*, 479–509.

Katz, L.C., and Shatz, C.J. (1996). Synaptic activity and the construction of cortical circuits. Science *274*, 1133–1138.

King, S.L., Marks, M.J., Grady, S.R., Caldarone, B.J., Koren, A.O., Mukhin, A.G., Collins, A.C., and Picciotto, M.R. (2003). Conditional expression in corticothalamic efferents reveals a developmental role for nicotinic acetylcholine receptors in modulation of passive avoidance behavior. J. Neurosci. *23*, 3837–3843.

Kumada, T., Jiang, Y., Kawanami, A., Cameron, D.B., and Komuro, H. (2009). Autonomous turning of cerebellar granule cells in vitro by intrinsic programs. Dev. Biol. *326*, 237–249.

Lund, R.D., Lund, J.S., and Wise, R.P. (1974). The organization of the retinal projection to the dorsal lateral geniculate nucleus in pigmented and albino rats. J. Comp. Neurol. *158*, 383–403.

McLaughlin, T., and O'Leary, D.D.M. (2005). Molecular gradients and development of retinotopic maps. Annu. Rev. Neurosci. *28*, 327–355.

McLaughlin, T., Torborg, C.L., Feller, M.B., and O'Leary, D.D. (2003). Retinotopic map refinement requires spontaneous retinal waves during a brief critical period of development. Neuron *40*, 1147–1160.

Meister, M., Wong, R.O.L., Baylor, D.A., and Shatz, C.J. (1991). Synchronous bursts of action potentials in ganglion cells of the developing mammalian retina. Science *252*, 939–943.

Moretti, M., Vailati, S., Zoli, M., Lippi, G., Riganti, L., Longhi, R., Viegi, A., Clementi, F., and Gotti, C. (2004). Nicotinic acetylcholine receptor subtypes expression during rat retina development and their regulation by visual experience. Mol. Pharmacol. *66*, 85–96.

Morishita, H., and Hensch, T.K. (2008). Critical period revisited: impact on vision. Curr. Opin. Neurobiol. *18*, 101–107.

Mrsic-Flogel, T.D., Hofer, S.B., Creutzfeldt, C., Cloëz-Tayarani, I., Changeux, J.P., Bonhoeffer, T., and Hübener, M. (2005). Altered map of visual space in the superior colliculus of mice lacking early retinal waves. J. Neurosci. *25*, 6921–6928.

Muir-Robinson, G., Hwang, B.J., and Feller, M.B. (2002). Retinogeniculate axons undergo eye-specific segregation in the absence of eye-specific layers. J. Neurosci. *22*, 5259–5264.

Mukhin, A.G., Gündisch, D., Horti, A.G., Koren, A.O., Tamagnan, G., Kimes, A.S., Chambers, J., Vaupel, D.B., King, S.L., Picciotto, M.R., et al. (2000). 5-Iodo-A-85380, an alpha4beta2 subtype-selective ligand for nicotinic acetylcholine receptors. Mol. Pharmacol. *57*, 642–649.

Nicol, X., Voyatzis, S., Muzerelle, A., Narboux-Nême, N., Südhof, T.C., Miles, R., and Gaspar, P. (2007). cAMP oscillations and retinal activity are permissive for ephrin signaling during the establishment of the retinotopic map. Nat. Neurosci. *10*, 340–347.

Penn, A.A., Riquelme, P.A., Feller, M.B., and Shatz, C.J. (1998). Competition in retinogeniculate patterning driven by spontaneous activity. Science *279*, 2108–2112.

Petros, T.J., Rebsam, A., and Mason, C.A. (2008). Retinal axon growth at the optic chiasm: to cross or not to cross. Annu. Rev. Neurosci. *31*, 295–315.

Pfeiffenberger, C., Cutforth, T., Woods, G., Yamada, J., Rentería, R.C., Copenhagen, D.R., Flanagan, J.G., and Feldheim, D.A. (2005). Ephrin-As and neural activity are required for eye-specific patterning during retinogeniculate mapping. Nat. Neurosci. *8*, 1022–1027.

Pfeiffenberger, C., Yamada, J., and Feldheim, D.A. (2006). Ephrin-As and patterned retinal activity act together in the development of topographic maps in the primary visual system. J. Neurosci. *26*, 12873–12884.

Plas, D.T., Lopez, J.E., and Crair, M.C. (2005). Pretarget sorting of retinocollicular axons in the mouse. J. Comp. Neurol. *491*, 305–319.

Rebsam, A., Petros, T.J., and Mason, C.A. (2009). Switching retinogeniculate axon laterality leads to normal targeting but abnormal eye-specific segregation that is activity dependent. J. Neurosci. *29*, 14855–14863.

Rossi, F.M., Pizzorusso, T., Porciatti, V., Marubio, L.M., Maffei, L., and Changeux, J.P. (2001). Requirement of the nicotinic acetylcholine receptor beta 2 subunit for the anatomical and functional development of the visual system. Proc. Natl. Acad. Sci. USA *98*, 6453–6458.

Shah, R.D., and Crair, M.C. (2008). Retinocollicular synapse maturation and plasticity are regulated by correlated retinal waves. J. Neurosci. *28*, 292–303.

Shatz, C.J. (2009). MHC class I: an unexpected role in neuronal plasticity. Neuron *64*, 40–45.

Shelly, M., Lim, B.K., Cancedda, L., Heilshorn, S.C., Gao, H., and Poo, M.M. (2010). Local and long-range reciprocal regulation of cAMP and cGMP in axon/dendrite formation. Science *327*, 547–552.

Shockett, P., Difilippantonio, M., Hellman, N., and Schatz, D.G. (1995). A modified tetracycline-regulated system provides autoregulatory, inducible gene expression in cultured cells and transgenic mice. Proc. Natl. Acad. Sci. USA *92*, 6522–6526.

Spitzer, N.C. (2006). Electrical activity in early neuronal development. Nature *444*, 707–712.

Stafford, B.K., Sher, A., Litke, A.M., and Feldheim, D.A. (2009). Spatial-temporal patterns of retinal waves underlying activity-dependent refinement of retinofugal projections. Neuron *64*, 200–212.

Stellwagen, D., and Shatz, C.J. (2002). An instructive role for retinal waves in the development of retinogeniculate connectivity. Neuron *33*, 357–367.

Stellwagen, D., Shatz, C.J., and Feller, M.B. (1999). Dynamics of retinal waves are controlled by cyclic AMP. Neuron *24*, 673–685.

Stryker, M.P., and Harris, W.A. (1986). Binocular impulse blockade prevents the formation of ocular dominance columns in cat visual cortex. J. Neurosci. *6*, 2117–2133.

Sun, C., Warland, D.K., Ballesteros, J.M., van der List, D., and Chalupa, L.M. (2008). Retinal waves in mice lacking the beta2 subunit of the nicotinic acetylcholine receptor. Proc. Natl. Acad. Sci. USA *105*, 13638–13643.

Tian, N., and Copenhagen, D.R. (2003). Visual stimulation is required for refinement of ON and OFF pathways in postnatal retina. Neuron *39*, 85–96.

Torborg, C.L., and Feller, M.B. (2004). Unbiased analysis of bulk axonal segregation patterns. J. Neurosci. Methods *135*, 17–26.

Torborg, C.L., Hansen, K.A., and Feller, M.B. (2005). High frequency, synchronized bursting drives eye-specific segregation of retinogeniculate projections. Nat. Neurosci. *8*, 72–78.

Visel, A., Thaller, C., and Eichele, G. (2004). GenePaint.org: an atlas of gene expression patterns in the mouse embryo. Nucleic Acids Res. *32* (Database issue), D552–D556.

Wang, L., Rangarajan, K.V., Lawhn-Heath, C.A., Sarnaik, R., Wang, B.S., Liu, X., and Cang, J. (2009). Direction-specific disruption of subcortical visual behavior and receptive fields in mice lacking the beta2 subunit of nicotinic acetylcholine receptor. J. Neurosci. *29*, 12909–12918.

Warland, D.K., Huberman, A.D., and Chalupa, L.M. (2006). Dynamics of spontaneous activity in the fetal macaque retina during development of retinogeniculate pathways. J. Neurosci. *26*, 5190–5197.

Wong, R.O. (1999). Retinal waves and visual system development. Annu. Rev. Neurosci. *22*, 29–47.

Xu, H.P., Chen, H., Ding, Q., Xie, Z.H., Chen, L., Diao, L., Wang, P., Gan, L., Crair, M.C., and Tian, N. (2010). The immune protein CD3zeta is required for normal development of neural circuits in the retina. Neuron *65*, 503–515.

Zheng, J., Lee, S., and Zhou, Z.J. (2006). A transient network of intrinsically bursting starburst cells underlies the generation of retinal waves. Nat. Neurosci. *9*, 363–371.